

Article

Photocatalytic Degradation of Phenol Using Chemical Vapor Deposition Graphene Column

Juhee Kim ^{1,†}, Baekwon Park ^{1,†}, Dong Heon Shin ^{1,†}, Je Min Yoo ^{1,2}, Hyukjin Lee ^{3,*} and Byung Hee Hong ^{1,4,*}

¹ Department of Chemistry, College of Natural Sciences, Seoul National University, Seoul 08826, Korea; juliejmom@snu.ac.kr (J.K.); pbk2640@snu.ac.kr (B.P.); t14713@snu.ac.kr (D.H.S.); Jyoo3487@bio-graphene.com (J.M.Y.)

² BIOGRAPHENE, 555 W 5th St 36th Floor, Los Angeles, CA 90013, USA

³ College of Pharmacy, Graduate School of Pharmaceutical Science, Ewha Womans University, Seoul 03760, Korea

⁴ Graphene Research Center, Advanced Institute of Convergence Technology, Suwon 16229, Korea

* Correspondence: hyukjin@ewha.ac.kr (H.L.); byunghee@snu.ac.kr (B.H.H.); Tel.: +82-2-3277-3026 (H.L.); +82-2-880-6569 (B.H.H.)

† These authors contributed equally to this work.

Received: 12 October 2020; Accepted: 28 October 2020; Published: 29 October 2020



Abstract: In the field of wastewater treatment, the advanced oxidation process (AOP) is a widely employed method. It uses reactive oxygen species (ROS) to degrade harmful organic and inorganic chemicals. Metal catalysts are the conventional standard when using these methods. However, they have drawbacks such as harsh activation conditions and poor recyclability. We previously suggested chemical vapor deposition (CVD) graphene film as an alternative metal-free catalyst. In this study, we enhanced the catalytic activity of the CVD graphene film by synergistically adding UV light irradiation. The result was complete degradation of phenol on a wafer-scale in a reduced timeframe. To further enhance the degradation process, we devised a graphene-based column for continuous in situ chemical oxidation and analyzed the intermediates over time, proving the potential of graphene-assisted AOP in industrial wastewater applications.

Keywords: CVD graphene; photocatalyst; advanced oxidation process; continuous phenol degradation; water treatment column

1. Introduction

As modern industrialization exacerbates environmental problems, studies related to ecological health are gaining traction across disciplines and geographies. Water pollution is especially detrimental to local and global health as it disrupts the clean water supply, the key to ecosystem mediation and balance. Much like the human body, clean water is essential to nurture native environments, and though pollutants can be naturally occurring, any number in excess can prove hugely detrimental to the well-being of the system. The pollutants of focus in this study are phenol and phenolic compounds. They are hazardous substances in industrial wastewater generated by plastics and petroleum refinement plants. Phenol is water-soluble, which means it travels in groundwater and is toxic to both the marine and terrestrial ecosystems at levels of just a few tens of ppm [1]. In humans, persisting dermal and pulmonary exposure to aqueous phenol toxins may lead to skin irritation, muscle weakness, and severe inflammation [2,3].

The advanced oxidation process (AOP) is used to treat toxic organic materials by oxidizing organic compounds with hydroxyl radicals ($\cdot\text{OH}$). Ferrous ion-based Fenton's reagent is commonly used to

complete the process; however, the reaction only activates in acidic conditions (pH 2.5–3.5) and requires additional steps to collect the purified water. In addition, the residual ferrous ions can cause DNA damage in humans through intracellular infusion and increase oxidative stress [4,5].

Until recently, graphene's application in wastewater treatment included only graphene oxides (GOs), or in combination with a complex with other materials. These forms of graphene catalyze the degradation of toxic organic pollutants [6,7], or in microbial fuel cells [8,9]. However, GOs exhibit limitations in commercialization because they require an additional metal catalyst.

Graphene as a nanomaterial is renowned for its superb physicochemical properties as well as its ability to fabricate into diverse sizes and forms. It is this flexibility that allows for its application in an assortment of research areas. Our group validated that a large-scale graphene film synthesized by the chemical vapor deposition (CVD) method could be used as a catalyst for organic acid degradation [10,11] used in wastewater treatment.

In the study, a monolayer graphene film generated hydroxyl radicals by accelerating the AOP of phenol and breaking down physisorbed hydrogen peroxide (H_2O_2) on its surface. This study reports an upgraded graphene catalyst which, when combined with UV irradiation, further expedites AOP. We enhanced the catalytic effects by constructing a graphene-coated column which allows for continuous phenol degradation. The column shows graphene's practicality when combined synergistically with UV light [12]. From the synthesis of graphene to the phenol degradation, all the processes carried out are environmentally friendly and cost-effective when compared to the previous wastewater catalysts and methods.

2. Results

2.1. Characterization of Graphene before and after Using as a Catalyst

Previous studies proved that graphene reduces hydrogen peroxide into hydroxyl radicals by temporarily forming a bond [13–16], which facilitates its functioning as an AOP catalyst [17,18]. Since UV light is also known to break hydrogen peroxide into hydroxyl radicals, we examined the combination of graphene and UV light as a method of catalytic enhancement. To ensure the integrity of its surface during the catalytic process, we examined the potential that either AOP or UV light could destroy the graphene structure (Figure 1a).

Raman spectroscopy provides the characteristic peaks for graphene where the G peak ($\sim 1590\text{ cm}^{-1}$) shows sp^2 bonded graphitic domain, and the D peak ($\sim 1390\text{ cm}^{-1}$) shows structural defects. Thus, the I_D/I_G value is a key indicator to represent graphene's structural integrity. The D peak observed in pristine graphene was barely visible, where the average value of I_D/I_G was 0.22 ± 0.03 . The I_D/I_G value of the same graphene samples used for the AOP experiment with and without UV irradiation displayed 0.21 ± 0.07 and 0.35 ± 0.04 , respectively, indicating little or no damages on the surface (Figure 1b). Also, to note was that the I_{2D}/I_G value stayed around 2, showing predominant monolayer coverage, and displaying the preserved integrity of graphene's surface and thus suggesting its recyclability (Figure 1c).

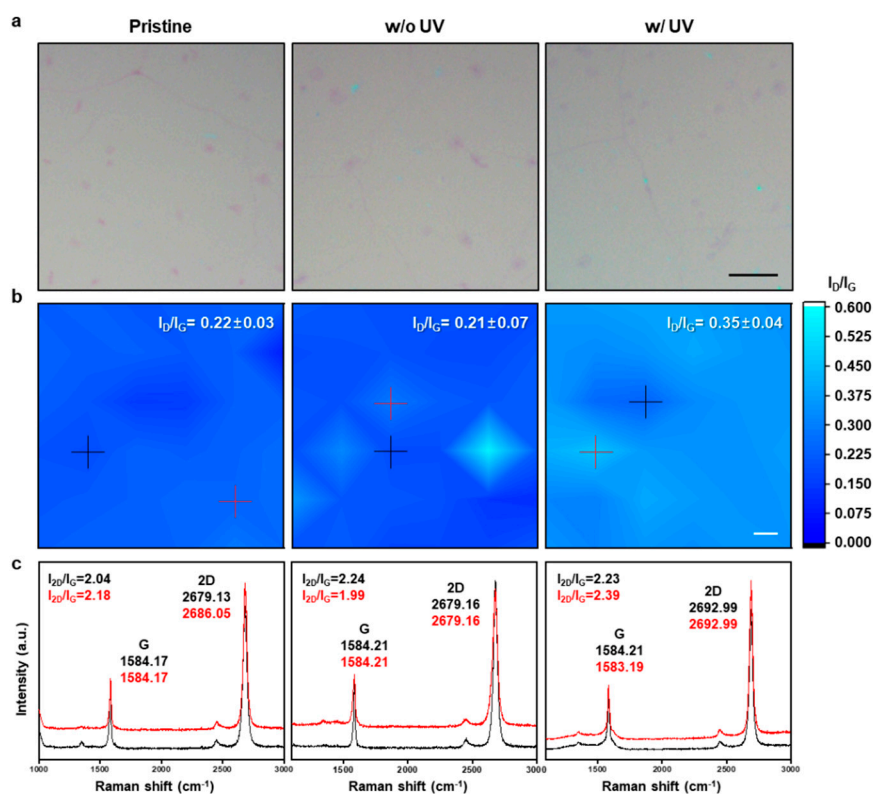


Figure 1. Characterization of graphene before and after usage. (a) Representative optical microscopic images of pristine graphene and graphene used for AOP with and without UV treatment. (Magnification $\times 1k$, scale bar $10 \mu\text{m}$) (b) Raman mapping of each graphene samples' I_D/I_G (Magnification $\times 500$, scale bar $1 \mu\text{m}$), and (c) representative Raman spectra.

2.2. UV Exposure Enhances the Catalytic Effect of Graphene on Phenol Degradation

The proposed mechanism of the enhanced catalytic effect of graphene by UV irradiation is illustrated in Figure 2a. Graphene assists the reduction of hydrogen peroxide, as well as the UV light, which both contribute to the adequate supply of hydroxyl radicals for phenol degradation. Due to UV light's ability to photolyze phenol directly [19], we validated the extent of its degradation as a factor of distance from the light source (Supplementary Materials, Figure S1). Even without hydrogen peroxide, UV light degraded 23.8% of phenol at a shorter distance (2 cm). This induced 10.4 times more degradation than the UV irradiated from further away (4 cm), while a negligible change in the concentration occurred in the absence of UV light. Therefore, to maximize the UV light's effect, we fixed the distance as 2 cm for the rest of the experiments.

We prepared a mixture of phenol and hydrogen peroxide solution, and a graphene film ($2 \times 2 \text{ cm}^2$) transferred on a SiO_2 wafer. From the control (CTL) sample, in the absence of graphene and UV light, there was negligible phenol degradation after three hours of incubation (Figure 2b). However, when introducing graphene and UV irradiation, the result was respectively 9.7% phenol degradation with graphene and 76.8% degradation with UV irradiation. Only when combined did graphene and UV treatment degrade phenol completely. The catalytic effect of graphene with UV exposure is analogous to that of the 0.05 mM Fenton's reagent, one of the most used AOP catalysts (Supplementary Materials, Figure S2). Although the degradation rate is slower, the graphene film is reusable without an additional process to remove the catalyst from the degraded mixture.

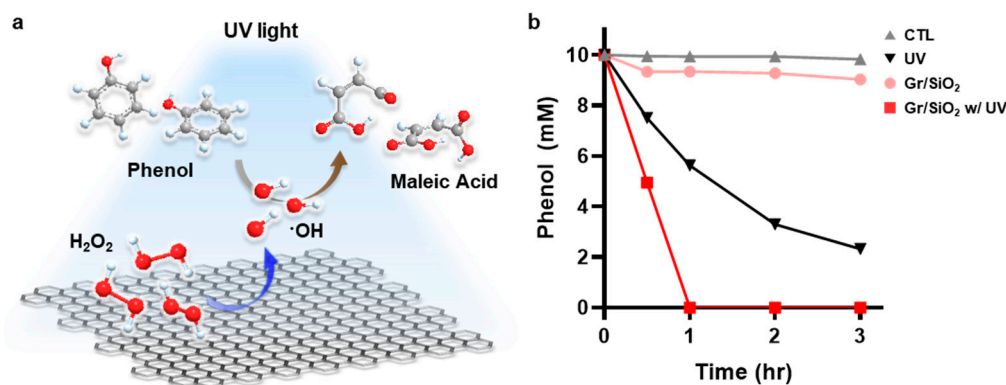


Figure 2. UV exposure enhances the catalytic effect of graphene on phenol degradation. (a) Schematic illustration of phenol degradation under UV exposure with graphene as the AOP catalyst. (b) Degradation of phenol by CTL (without graphene and UV), UV (UV irradiation), Gr/SiO₂ (graphene), and Gr/SiO₂ w/UV (graphene with UV irradiation) within three hours.

2.3. Continuous Degradation of Phenol Using a Graphene Column

Graphene is bendable when transferred onto a flexible surface. This flexibility allows for the construction of a graphene-coated column with UV-resistant polyimide (PI) film as the substrate (Figure 3a) [20]. Before assembling the column, we verified whether phenol could adhere to either surface, as phenol can interact with graphene and PI through π - π interactions [21] (Supplementary Materials, Figure S3). When floating the PI film on phenol solution for three hours, there was almost no change in concentration. However, following the introduction of $2 \times 2 \text{ cm}^2$ graphene, transferred on the PI film (Gr/PI), we detected a slight reduction, of which the change was continuously negligible.

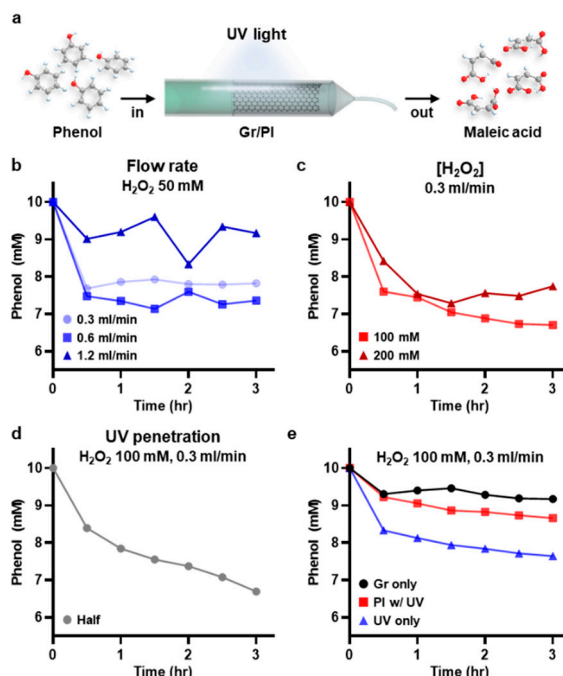


Figure 3. Optimizations of continuous phenol degradation by the graphene column. (a) Schematic drawing of the graphene column. The optimal condition of graphene column was found by comparing the effect of (b) flow rate of solution (10 mM phenol and 50 mM H₂O₂), (c) concentration of H₂O₂ at a fixed flow rate of 0.3 mL/min, and (d) the extent of graphene's column coverage. (e) The synergistic effect of graphene and UV light treatment is considerable compared to either graphene or UV light treatment.

Whether the substrate change could affect graphene's catalytic ability was validated by transferring graphene $2 \times 2 \text{ cm}^2$ on the PI film. Despite the substrate change, phenol was 17.7% degraded by Gr/PI (Supplementary Materials, Figure S4). However, as PI can interfere with UV penetration, when we floated the sample so that the graphene faces down, the synergistic introduction of UV light degraded phenol of only 51.2%, displaying decreased catalytic activity comparison with Gr/SiO₂. Since the UV irradiation nonetheless improved the degradation efficiency, we increased the dimension of graphene film on PI and rolled it into a glass column so that graphene covers the inside of the column entirely. We used a syringe pump connected to one end of the column and injected the phenol solution at a constant flow rate while the degraded product was collected from the other end. The whole process of the graphene column experiment is described in Video S1.

Of various possibilities, the evaluated factors include the flow rate, hydrogen peroxide concentration, and UV penetration through PI on phenol degradation [22]. First, we fixed the hydrogen peroxide concentration to 50 mM, and controlled the flow rate (Figure 3b). At the fastest flow rate, 1.2 mL/min was the minimum catalytic activity, as it only allows the short exposure time to graphene and UV light. While the flow rate of 0.6 mL/min achieved the maximum performance, there was a lurking factor of syringe replacement during the experiment. By employing the flow rate of 0.3 mL/min, the final phenol concentration was similar to 0.6 mL/min without additional changes. On average, the flow rate resulted in 21.8% of constant phenol degradation, despite the incoming of new phenol, suggesting an optimal flow rate of 0.3 mL/min for ensuing experiments.

As hydrogen peroxide can naturally reduce to water and oxygen, increasing its concentration does not pose serious concern. At the flow rate of 0.3 mL/min, 100 mM of hydrogen peroxide yielded the most favorable outcome (Figure 3c). Since we obtained the experiment's maximum efficiency at the flow rate of 0.3 mL/min and 100 mM of hydrogen peroxide, we set these variables as the optimized condition.

Regarding the UV light blockage by PI film, we validated the degradation efficiency with only the lower half of the column covered with graphene (Figure 3d). The degradation rate was slower when using smaller graphene; however, the final concentration of phenol was saturated to around 6.7 mM. The efficiency is nearly equivalent to that obtained with full graphene coverage, suggesting that graphene size is a more critical factor than the amount of UV penetration.

In accordance with Gr/SiO₂, the graphene column's degradation efficiency was highest in the combination of graphene and UV light. Respectively, phenol degraded around 8.3% with graphene and 23.6% under UV irradiation (Figure 3e). When the PI film was rolled into the column and introduced UV light, 13.4% was degraded. Therefore, considering the blockage of UV light penetration by PI substrate, a considerable synergistic effect between graphene and UV led to improved catalytic efficiency.

Persistent UV irradiation increased the column's temperature to around 60–70 °C, whereas the outflowing solution remained around room temperature (Supplementary Materials, Figure S5a). To verify the sole effect of increased temperature on degradation, we incubated phenol at 60 °C in the presence of Gr/SiO₂ (Supplementary Materials, Figure S5b) [23]. While the increased temperature degraded 20.8% of phenol, which is better than Gr/SiO₂ at room temperature, the efficiency was significantly lower than the combined treatment of Gr/SiO₂ and UV.

In order to improve efficiency, we connected two graphene columns in series and introduced UV light (Supplementary Materials, Figure S6a). Although we observed a slower catalytic efficiency at the earlier time point, overall, 36.9% phenol was degraded at the three-hour mark (Supplementary Materials, Figure S6b). Compared to the one column system, even better efficiency was observed beyond two hours, expecting the doubled volume of safely treated phenol.

2.4. Evaluation of Intermediates from the AOP of Phenol

From the two-column system, we detected and analyzed various AOP intermediates in chronological order. We compared the retention time and UV spectrum of each organic acids and illustrated the phenol's degradation pathway (Figure 4a). From the beginning to 30 min of UV

exposure, we identified hydroquinone (HQ) and dihydroxy benzene (DB), the very first intermediates formed by the attack of hydroxyl radical on phenol (Figure 4b). The concentration of DB increased until an hour later, where we started to observe muconic acid (MU). An hour and a half later, we consistently detected *p*-benzoquinone (*p*-BQ), the oxidized product of HQ, and maleic acid (MA), the final product of phenol degradation, until the three-hour mark.

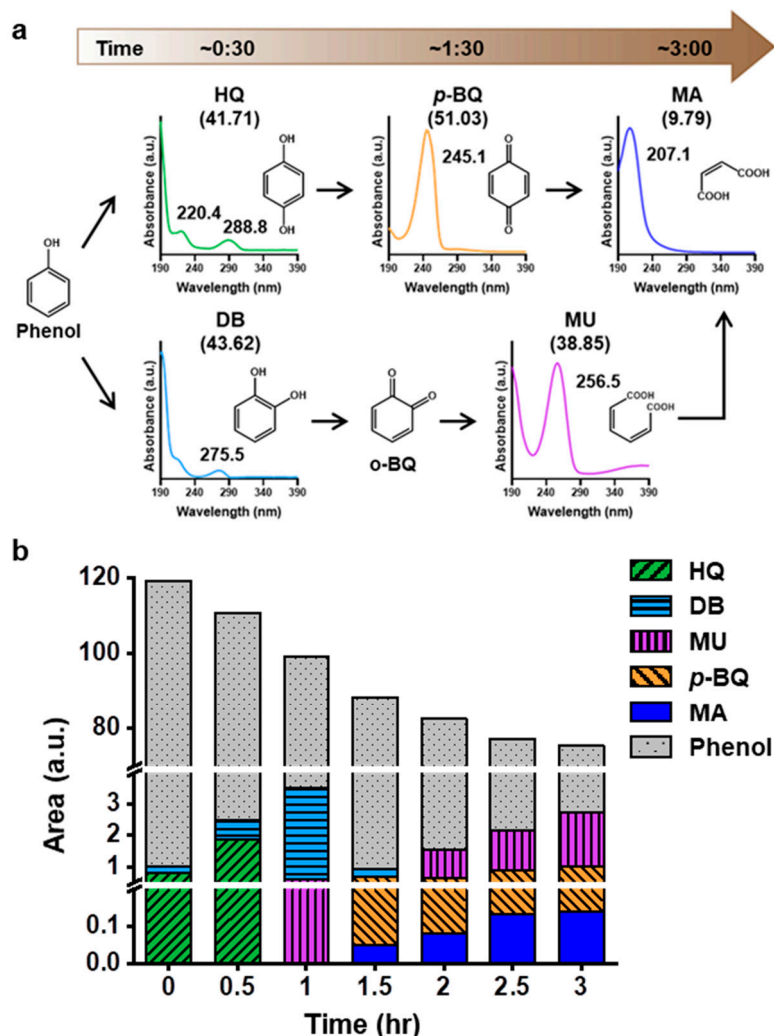


Figure 4. Analysis of oxidized derivatives from phenol. (a) Summarized diagram of the phenol degradation process with the UV spectra of intermediates detected at each retention time and experimental time point. (b) The change in the area under the HPLC curve of phenol and each intermediate.

Interestingly, from the combination of Gr/SiO₂ and UV irradiation, we only examined DB and MU, and within two hours, even these intermediates became undetectable (Supplementary Materials, Figure S7a). Unlike the intermediate analysis by the graphene column, HQ was not examined from the Gr/SiO₂ sample due to its rapid oxidation. However, the same intermediates were constantly identified until the three-hour mark with Fenton's reagent (Supplementary Materials, Figure S7b). Therefore, graphene with UV treatment can be deemed a promising catalyst for safer phenol degradation treatment.

While we analyzed other phenol-degraded intermediates by the purchased products, MU was confirmed by the reaction of DB and Fenton's reagent (Supplementary Materials, Figure S7b). The oxidation of DB produces subsequent intermediates, including *cis,cis*-muconic acid [24,25]. By comparing the UV spectrum and retention time, we concluded that the intermediate at timepoint 38–39 min of the high-performance liquid chromatography (HPLC) spectrum matches MU.

3. Discussion

In this study, we enhanced graphene's catalytic effect in phenol degradation through AOP by introducing a synergistic UV treatment. We achieved the continuous degradation of phenol using a customized graphene column along with optimized conditions such as the flow rate and adjusted the concentration of hydrogen peroxide. The intermediates from the degraded phenol were analyzed by HPLC and UV spectra, showing the phenol's conventional degradation process. Compared to Fenton's reagent, graphene film can be activated under relatively mild conditions. In addition, the use of graphene film does not require additional steps for salt removal or water collection, making it a cost-effective and environmentally friendly AOP catalyst.

This work's objective was to develop a hydroxyl radical generation method as once the radicals are made, they react non-selectively with phenol and the intermediates at near diffusion-controlled rates [26,27]. Graphene with UV irradiation synergistically functioned as the catalyst for hydrogen peroxide splitting, resulting in the enhancement of phenol's AOP. TiO₂ is a standard photocatalyst, in which Evonik P25 has been reported to completely degrade phenol 25 ppm in 400 min [28], and TiO₂-coated quartz tube could degrade phenol of 100 mg/L within 4 h under UV irradiation [29]. Compared to both cases, the initial phenol concentration we used in this study (941.1 mg/L, 941 ppm) is much higher, showing a better catalytic efficiency. Although the graphene column only degraded 33% of phenol, the initial phenol concentration was much higher than that of normal polluted water [3,30]. Therefore, we expect a better catalytic effect of graphene and UV treatment at more average phenol concentrations. Doping graphene with nitrogen can improve the catalytic activity as electronegative nitrogen favorably changes the electron density of the graphitic domain, thus producing more active sites for more hydroxyl radical generation [15,31]. Increasing graphene's surface area or repeating the degradation process can also lead to enhanced phenol degradation.

Beyond the possibility of AOP catalyzation, graphene's superb physicochemical properties make it an ideal candidate for other wastewater treatment processes. As suggested previously, GOs or reduced GOs can effectively adsorb pesticides through π - π interactions and due to their large surface area [32,33]. In addition, nanoporous graphene can selectively transport specific ions for further treatments [34]. Graphene can also be applied for water desalination, thanks to its high salt rejection rate and anti-fouling capability [35]. Therefore, with appropriate modifications depending on intended use, the continuous graphene column system promises wholesome innovations across many processes of commercial water treatment.

4. Materials and Methods

4.1. Synthesis and Characterization of Graphene

Graphene was synthesized using a chemical vapor deposition method based on the previous research [36]. Cu foil (99.95%, Alfa Aesar, Haverhill, MA, USA) was rolled in a quartz tube and annealed for 90 min while increasing temperature up to 1000 °C at the maximum rate while flowing 10 sccm H₂. The graphene synthesis was done by flowing 70 sccm CH₄ at 1000 °C for 30 min, followed by rapid cooling. On one side of the Cu foil, the prepared PMMA solution (poly(methyl methacrylate) (182265-500G, Sigma Aldrich, St. Louis, MO, USA) dissolved in chlorobenzene (319996-2.5 L, Sigma Aldrich, St. Louis, MO, USA) was spin-coated on one side for protection, and the synthesized graphene on other side was removed through reactive ion etching. Then, in order to dissolve Cu, we floated the Cu foil on the 100 mM ammonium persulfate aqueous solution (248614-2.5KG, Sigma Aldrich, St. Louis, MO, USA), after which we rinsed with deionized (DI) water. The graphene was then transferred onto either SiO₂/Si wafer or PI film (PI-Film 0.05t, Alphaflon, Seoul, South Korea). Right before using the graphene, PMMA was removed by acetone to prevent oxidation.

4.2. Degradation of Phenol Using Graphene Transferred on a Wafer or PI Film

Graphene was cut by the size of $2 \times 2 \text{ cm}^2$ and transferred on to the SiO_2/Si wafer or the PI film. PMMA was removed right before its usage to prevent oxidation. The mixture of phenol 10 mM (328111, Sigma Aldrich, St. Louis, MO, USA) and H_2O_2 100 mM (34.5%, 092817, Samchun, Seoul, South Korea) aqueous solution was prepared and kept immersed in darkness. In a glass petri dish, the graphene and 5 mL of the solution were added, and 200 μL of the solution was aliquoted every hour for three hours. UV ozone cleaner (UVC-300, Omniscience, Yongin, South Korea) was used as the UV light source, of which the wavelength is 184.9 and 253.7 nm.

4.3. Comparison with Fenton's Reagent

Fenton's reagent was prepared by making an aqueous solution of Iron(II) sulfate heptahydrate (215422-5G, Sigma Aldrich, St. Louis, MO, USA) at the final concentration of 0.05 mM to compare its catalytic activity with graphene. The final concentration of phenol and H_2O_2 was the same as mentioned in Section 4.2. In a glass petri dish, 5 mL of the solution was added, and without the exposure to UV light, aliquoted 200 μL of solution every hour for three hours.

4.4. Temperature Measurement

The solution flowing out from the column was collected in a 20 mL vial, which was replaced every 30 min. The temperature of the column inside the UV ozone cleaner and the solution gathered in the vial was measured by an infrared thermometer.

4.5. Graphene Column

Graphene of size $6 \times 11.5 \text{ cm}^2$ was transferred on a PI film, and after removal of PMMA, it was rolled inside a quartz column. The phenol solution was prepared as described in Section 4.2. Around 50 mL of the solution was filled inside the column, connected to the 50 mL syringe filled with the same solution. After placing the column inside the UV equipment, the flow rate was set by a syringe pump (KDS101 Legacy syringe pump, 78-1101, kdScientific, Holliston, MA, USA). The solution flowing out of the column was aliquoted every 30 min for three hours.

4.6. Raman Spectroscopy

The surface integrity of graphene before and after using it as a catalyst was detected by Raman spectroscopy (Renishaw, Wotton-under-Edge, UK) with a 514 nm laser. Graphene transferred on a SiO_2/Si wafer was used for the measurement.

4.7. High-Performance Liquid Chromatography

Degradation of phenol was detected through HPLC (Ultimate3000, Thermo Dionex, Sunnyvale, CA, USA). Hydroquinone (H9003-100G), 1,2-dihydroxybenzene (135011-5G), *p*-Benzoquinone (B10358-5G), and maleic acid (M0375-100G), all from Sigma Aldrich, St. Louis, MO, USA, were dissolved in DI water for HPLC analysis. The monochromatic light wavelength was set as 280 nm and Chromeleon software (Version 6.80, Dionex Corporation, Sunnyvale, CA, USA) used for data analysis.

4.8. Dihydroxybenzene Reaction with Fenton's Reagent

An aqueous solution of dihydroxybenzene 10 mM was mixed with Fenton's reagent 0.05 mM and H_2O_2 100 mM. The reaction proceeded immediately, followed by HPLC analysis.

Supplementary Materials: The following are available online at <http://www.mdpi.com/2073-4344/10/11/1251/s1>, Figure S1: The intensity of UV light's illumination affects the extent of phenol degradation, Figure S2: Comparison of the graphene's catalytic effect on Fenton's reagent, Figure S3: Adhesion of phenol on graphene or PI surface does not significantly reduce the phenol concentration, Figure S4: Graphene transferred on PI film still exhibits the catalytic effect, Figure S5: The effect of temperature on phenol degradation, Figure S6: The two-column system for the improvement in degradation efficiency, Figure S7: The AOP intermediates detected when using graphene and Fenton's reagent, Video S1: Continuous degradation of phenol using the CVD graphene column.

Author Contributions: J.K., B.P., and D.H.S. conceptualized, designed models, operated experiments, validated the data, and contributed to writing. J.M.Y. reviewed and edited the article. H.L. and B.H.H. administered and supervised the project. All authors have read and agreed to the published version of the manuscript.

Funding: This work was supported by National Research Foundation of Korea (NRF) with grant funded by the Korean Government (NRF-2019-Global Ph.D. Fellowship Program), and by NRF with grant number of (2018R1A5A2025286) and (2020R1A2C2004364).

Acknowledgments: The authors acknowledge J.P. Hostetler for assisting in manuscript completion and revision.

Conflicts of Interest: The authors declare no conflict of interest.

References

1. Duan, W.; Meng, F.; Lin, Y.; Wang, G. Toxicological effects of phenol on four marine microalgae. *Environ. Toxicol. Pharmacol.* **2017**, *52*, 170–176. [[CrossRef](#)] [[PubMed](#)]
2. Hayati, F.; Isari, A.A.; Fattahi, M.; Anvaripour, B.; Jorfi, S. Photocatalytic decontamination of phenol and petrochemical wastewater through ZnO/TiO₂ decorated on reduced graphene oxide nanocomposite: Influential operating factors, mechanism, and electrical energy consumption. *RSC Adv.* **2018**, *8*, 40035–40053. [[CrossRef](#)]
3. Michałowicz, J.; Duda, W. Phenols—Sources and Toxicity. *Pol. J. Environ. Stud.* **2007**, *16*, 347–362.
4. Solís-López, M.; Durán-Moreno, A.; Rigas, F.; Morales, A.A.; Navarrete, M.; Ramírez-Zamora, R.M. 9—Assessment of copper slag as a sustainable fenton-type photocatalyst for water disinfection. In *Water Reclamation and Sustainability*; Ahuja, S., Ed.; Elsevier: Boston, MA, USA, 2014; pp. 199–227. [[CrossRef](#)]
5. Su, P.; Zhou, M.; Lu, X.; Yang, W.; Ren, G.; Cai, J. Electrochemical catalytic mechanism of N-doped graphene for enhanced H₂O₂ yield and in-situ degradation of organic pollutant. *Appl. Catal. B* **2019**, *245*, 583–595. [[CrossRef](#)]
6. Raut-Jadhav, S.; Bagal, M.V. 5—Advanced graphene-transition metal-oxide-based nanocomposite photocatalysts for efficient degradation of pollutants present in wastewater. In *Multifunctional Nanostructured Metal Oxides for Energy Harvesting and Storage Devices*; Vijay, B.P., Paresh, H.S., Bhanvase, B.A., Eds.; CRC Press: Boca Raton, FL, USA, 2020. [[CrossRef](#)]
7. Wu, Y.; Luo, H.; Wang, H.; Zhang, L.; Liu, P.; Feng, L. Fast adsorption of nickel ions by porous graphene oxide/sawdust composite and reuse for phenol degradation from aqueous solutions. *J. Colloid Interface Sci.* **2014**, *436*, 90–98. [[CrossRef](#)] [[PubMed](#)]
8. Sun, M.; Liu, H.; Liu, Y.; Qu, J.; Li, J. Graphene-based transition metal oxide nanocomposites for the oxygen reduction reaction. *Nanoscale* **2015**, *7*, 1250–1269. [[CrossRef](#)] [[PubMed](#)]
9. Yuan, H.; Hou, Y.; Abu-Reesh, I.M.; Chen, J.; He, Z. Oxygen reduction reaction catalysts used in microbial fuel cells for energy-efficient wastewater treatment: A review. *Mater. Horiz.* **2016**, *3*, 382–401. [[CrossRef](#)]
10. Yoo, J.M.; Park, B.; Kim, S.J.; Choi, Y.S.; Park, S.; Jeong, E.H.; Lee, H.; Hong, B.H. Catalytic degradation of phenols by recyclable CVD graphene films. *Nanoscale* **2018**, *10*, 5840–5844. [[CrossRef](#)]
11. Rocha, R.P.; Gonçalves, A.G.; Pastrana-Martínez, L.M.; Bordoni, B.C.; Soares, O.S.G.P.; Órfão, J.J.M.; Faria, J.L.; Figueiredo, J.L.; Silva, A.M.T.; Pereira, M.F.R. Nitrogen-doped graphene-based materials for advanced oxidation processes. *Catal. Today* **2015**, *249*, 192–198. [[CrossRef](#)]
12. Ge, L.; Li, H.; Du, X.; Zhu, M.; Chen, W.; Shi, T.; Hao, N.; Liu, Q.; Wang, K. Facile one-pot synthesis of visible light-responsive BiPO₄/nitrogen doped graphene hydrogel for fabricating label-free photoelectrochemical tetracycline aptasensor. *Biosens. Bioelectron.* **2018**, *111*, 131–137. [[CrossRef](#)]
13. Tian, G.-L.; Zhao, M.-Q.; Yu, D.; Kong, X.-Y.; Huang, J.-Q.; Zhang, Q.; Wei, F. Nitrogen-Doped Graphene/Carbon Nanotube Hybrids: In Situ Formation on Bifunctional Catalysts and Their Superior Electrocatalytic Activity for Oxygen Evolution/Reduction Reaction. *Small* **2014**, *10*, 2251–2259. [[CrossRef](#)]

14. Wang, Z.; Lv, X.; Weng, J. High peroxidase catalytic activity of exfoliated few-layer graphene. *Carbon* **2013**, *62*, 51–60. [[CrossRef](#)]
15. Wu, P.; Du, P.; Zhang, H.; Cai, C. Microscopic effects of the bonding configuration of nitrogen-doped graphene on its reactivity toward hydrogen peroxide reduction reaction. *Phys. Chem. Chem. Phys.* **2013**, *15*, 6920–6928. [[CrossRef](#)]
16. Garg, B.; Bisht, T.; Ling, Y.-C. Graphene-Based Nanomaterials as Efficient Peroxidase Mimetic Catalysts for Biosensing Applications: An Overview. *Molecules* **2015**, *20*, 14155–14190. [[CrossRef](#)]
17. Fu, C.-C.; Juang, R.-S.; Huq, M.M.; Hsieh, C.-T. Enhanced adsorption and photodegradation of phenol in aqueous suspensions of titania/graphene oxide composite catalysts. *J. Taiwan Inst. Chem. Eng.* **2016**, *67*, 338–345. [[CrossRef](#)]
18. Wang, Q.; Li, H.; Yang, J.-H.; Sun, Q.; Li, Q.; Yang, J. Iron phthalocyanine-graphene donor-acceptor hybrids for visible-light-assisted degradation of phenol in the presence of H₂O₂. *Appl. Catal. B* **2016**, *192*, 182–192. [[CrossRef](#)]
19. Prasse, C.; Ford, B.; Nomura, D.K.; Sedlak, D.L. Unexpected transformation of dissolved phenols to toxic dicarbonyls by hydroxyl radicals and UV light. *Proc. Natl. Acad. Sci. USA* **2018**, *115*, 2311–2316. [[CrossRef](#)]
20. Papageorgiou, D.G.; Kinloch, I.A.; Young, R.J. Mechanical properties of graphene and graphene-based nanocomposites. *Prog. Mater. Sci.* **2017**, *90*, 75–127. [[CrossRef](#)]
21. Tran, T.M.H.; Ambrosi, A.; Pumera, M. Phenols as probes of chemical composition of graphene oxide. *Phys. Chem. Chem. Phys.* **2016**, *18*, 30515–30519. [[CrossRef](#)]
22. Meshram, S.; Limaye, R.; Ghodke, S.; Nigam, S.; Sonawane, S.; Chikate, R. Continuous flow photocatalytic reactor using ZnO–bentonite nanocomposite for degradation of phenol. *Chem. Eng. J.* **2011**, *172*, 1008–1015. [[CrossRef](#)]
23. Magerusan, L.; Socaci, C.; Pogacean, F.; Rosu, M.C.; Biris, A.R.; Coros, M.; Turza, A.; Floare-Avram, V.; Katona, G.; Pruneanu, S. Enhancement of peroxidase-like activity of N-doped graphene assembled with iron-tetrapyridylporphyrin. *RSC Adv.* **2016**, *6*, 79497–79506. [[CrossRef](#)]
24. M'hemdi, A.; Dbira, B.; Abdelhedi, R.; Brillas, E.; Ammar, S. Mineralization of Catechol by Fenton and Photo-Fenton Processes. *CLEAN Soil Air Water* **2012**, *40*, 878–885. [[CrossRef](#)]
25. Coupé, F.; Petitjean, L.; Anastas, P.T.; Caijo, F.; Escande, V.; Darcel, C. Sustainable oxidative cleavage of catechols for the synthesis of muconic acid and muconolactones including lignin upgrading. *Green Chem.* **2020**, *22*, 6204–6211. [[CrossRef](#)]
26. Li, W.; Jain, T.; Ishida, K.; Liu, H. A mechanistic understanding of the degradation of trace organic contaminants by UV/hydrogen peroxide, UV/persulfate and UV/free chlorine for water reuse. *Environ. Sci. Water Res. Technol.* **2017**, *3*, 128–138. [[CrossRef](#)]
27. Appiani, E.; Page, S.E.; McNeill, K. On the Use of Hydroxyl Radical Kinetics to Assess the Number-Average Molecular Weight of Dissolved Organic Matter. *Environ. Sci. Technol.* **2014**, *48*, 11794–11802. [[CrossRef](#)]
28. Bianchi, C.L.; Stucchi, M.; Pirola, C.; Cerrato, G.; Morandi, S.; Sacchi, B.; Vitali, S.; Michele, A.D.; Capucci, V. Micro-sized TiO₂ catalyst in powder form and as coating on porcelain grès tile for the photodegradation of phenol as model pollutant for water phase. *Adv. Mater. Sci.* **2017**, *2*. [[CrossRef](#)]
29. Suzuki, H.; Araki, S.; Yamamoto, H. Evaluation of advanced oxidation processes (AOP) using O₃, UV, and TiO₂ for the degradation of phenol in water. *J. Water Process. Eng.* **2015**, *7*, 54–60. [[CrossRef](#)]
30. ATSDR. *Toxicological Profile for Phenol*; U.S. Department of Health and Human Services, Public Health Service: Atlanta, GA, USA, 2008; pp. 149–172.
31. Pogacean, F.; Socaci, C.; Pruneanu, S.; Biris, A.R.; Coros, M.; Magerusan, L.; Katona, G.; Turcu, R.; Borodi, G. Graphene based nanomaterials as chemical sensors for hydrogen peroxide—A comparison study of their intrinsic peroxidase catalytic behavior. *Sens. Actuators B Chem.* **2015**, *213*, 474–483. [[CrossRef](#)]
32. Maliyekkal, S.M.; Sreepasad, T.S.; Krishnan, D.; Kouser, S.; Mishra, A.K.; Waghmare, U.V.; Pradeep, T. Graphene: A Reusable Substrate for Unprecedented Adsorption of Pesticides. *Small* **2013**, *9*, 273–283. [[CrossRef](#)] [[PubMed](#)]
33. Yang, K.; Wang, J.; Chen, X.; Zhao, Q.; Ghaffar, A.; Chen, B. Application of graphene-based materials in water purification: From the nanoscale to specific devices. *Environ. Sci. Nano* **2018**, *5*, 1264–1297. [[CrossRef](#)]
34. Bodzek, M.; Konieczny, K.; Kwiecińska-Mydlak, A. Nanotechnology in water and wastewater treatment. Graphene—the nanomaterial for next generation of semipermeable membranes. *Crit. Rev. Environ. Sci. Technol.* **2020**, *50*, 1515–1579. [[CrossRef](#)]

35. Seo, D.H.; Pineda, S.; Woo, Y.C.; Xie, M.; Murdock, A.T.; Ang, E.Y.M.; Jiao, Y.; Park, M.J.; Lim, S.I.; Lawn, M.; et al. Anti-fouling graphene-based membranes for effective water desalination. *Nat. Commun.* **2018**, *9*, 683. [[CrossRef](#)] [[PubMed](#)]
36. Bae, S.; Kim, H.; Lee, Y.; Xu, X.; Park, J.-S.; Zheng, Y.; Balakrishnan, J.; Lei, T.; Ri Kim, H.; Song, Y.I.; et al. Roll-to-roll production of 30-inch graphene films for transparent electrodes. *Nat. Nanotechnol.* **2010**, *5*, 574–578. [[CrossRef](#)]

Publisher’s Note: MDPI stays neutral with regard to jurisdictional claims in published maps and institutional affiliations.



© 2020 by the authors. Licensee MDPI, Basel, Switzerland. This article is an open access article distributed under the terms and conditions of the Creative Commons Attribution (CC BY) license (<http://creativecommons.org/licenses/by/4.0/>).